Bain transformation in Cu_xPd_{1-x} ($x \sim 0.5$) alloys: An embedded-atom study

M. G. Donato, P. Ballone, and P. V. Giaquinta
Istituto Nazionale per la Fisica della Materia, 98166 Messina, Italy
and Dipartimento di Fisica, Universitá degli Studi di Messina, Contrada Papardo, Casella Postale 50, 98166 Messina, Italy
(Received 30 April 1999; revised manuscript received 17 August 1999)

We investigate the B2 to random-fcc structural transformation in Cu_xPd_{1-x} alloys as a function of concentration around $x=0.5$. The system is modeled by the embedded atom method (EAM), and its free energy is computed by Monte Carlo simulation in the isothermal-isobaric ensemble. Our results show that the temperature stability range for the B2 phase is estimated correctly by the EAM model, while the x dependence of the transformation temperature around the stoichiometric composition ($x=0.5$) is not well reproduced.

INTRODUCTION

The interplay of electronic and thermal effects in solid metallic alloys gives rise to a surprising variety of different phases, whose stability boundaries are often difficult to locate accurately both by experiments and by theoretical methods.

In our study we test the ability of a simple model [the embedded atom model (EAM)[1]] to identify the concentration and temperature stability range for the ordered B2 phase of the Cu_xPd_{1-x} alloy. On cooling from the liquid state, Cu_xPd_{1-x} crystallizes in a continuous solid solution, based on the fcc lattice. At low temperature, the phase diagram displays several intermetallic phases, of which the ordered $L1_2$ (at $x \sim 0.75$) and B2 (at $x \sim 0.5$) structures are the most prominent ones.[2] We focus on the transformation that gives rise to this second phase (i.e., the B2), which involves the simultaneous order/disorder and structural transitions.

We find that the EAM predicts a temperature range for the stability of the B2 structure in fair agreement with the experimental data. However, this model is unable to account for the large asymmetry of the B2 stability region with respect to the stoichiometric ($x=0.5$) composition, that is observed in the experimental phase diagram. The comparison with previous *ab-initio* computations[3] allows us to understand both the reasons for the agreement and the disagreement between the computational results and the experimental data.

THE COMPUTATIONAL METHOD

The embedded atom method provides the simplest model to describe the metallic bonding of transition and post-transition metals. We adopt the original approach, introduced in Ref. 1, together with the explicit parametrization of Ref. 4 for the Cu-Pd potential. Here we simply remind that the potential energy E as a function of the atomic coordinates $\{\mathbf{R_I}; (I=1,N)\}$ is written as

$$E[\mathbf{R_I}] = \frac{1}{2}\sum_{I\neq J} \phi_{IJ}(|\mathbf{R_I}-\mathbf{R_J}|) + \sum_I F_I[\rho(\mathbf{R_I})], \qquad (1)$$

where ϕ_{IJ} is a repulsive pair potential, and $F_I[\rho(\mathbf{R_I})]$ is the energy gain in embedding the atom I into the valence charge density $\rho(\mathbf{R_I})$. In turn, $\rho(\mathbf{R})$ is given by the superposition of all the valence electron distributions associated to each atom in the system. The indexes I and J on ϕ_{IJ} and F_I indicate that these functions depend on the type (Cu or Pd) of the atoms involved.

The repulsive potential ϕ and the embedding function F are devised in order to reproduce the ground-state structure, and to fit the elastic properties and vacancy formation energies of the pure elements. One additional parameter in the embedding part determines the mixing enthalpy of the alloys. In the case of the Cu-Pd system, the mixing is exothermic, i.e., the cohesive energy is increased by hetero-coordination of Cu and Pd in the alloy.

To sample the phase space of the system, we use the Monte Carlo algorithm in the isothermal-isobaric ensemble.[5] All simulations are performed at zero pressure. The unconstrained variation of all the parameters defining the simulation cell sometimes makes it difficult to identify the resulting structures, especially at high temperatures, for which shape fluctuations can be large. To circumvent this problem, we explore the phase diagram by a series of simulations in which the system volume is allowed to change at fixed shape of the simulation cell.[6] This constraint extends the (meta-) stability of each structure up to the melting point, and allows us to compute the free energy of each solid phase over a wide temperature range. This computation is complemented by a series of unconstrained isothermal-isobaric runs,[7] in order to check the ability of the system to transform from one metastable phase to the stable one, and to rule out the presence of unexpected structures.

Since the order-disorder transition is a crucial component of the phase transformation, and inter-diffusion does not occur in the solid phase during runs of practical length, we sample the atomic exchange processes by attempting to swap the position of a pair of atoms chosen at random and belonging to the two different atomic species.

Simulations are performed for samples of 1024 atoms, within a cubic cell in the case of the B2 phase, and a tetragonal cell with $c/a=\sqrt{2}$ for the disordered fcc solution. This value for the c/a ratio has been chosen in such a way that the two simulation cells are related by the well-known Bain transformation between the bcc and the fcc structures.[8] Most runs extend over 10^7 single atom moves,[9] with volume

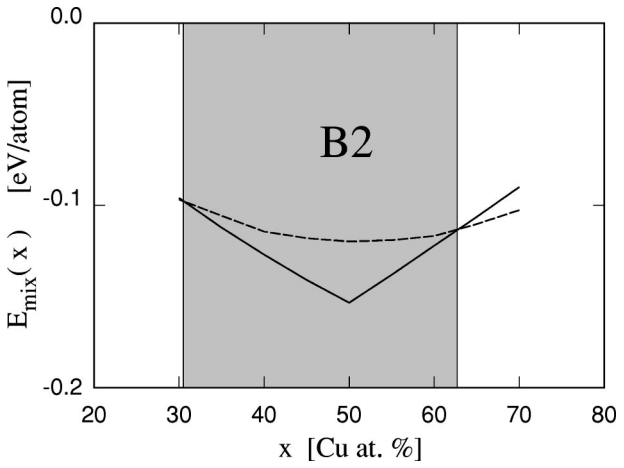

FIG. 1. Excess energy of mixing (see text) at $T=0$ K for the ordered B2 (full line) and disordered fcc (dash line) phases as a function of concentration. The shading identifies the stability range for the B2 phase.

changes and atom pairs interchanges attempted, on average, every 200 single atom steps. Thermal averages are accumulated over the last 4 10^6 steps of the runs. In most cases, the statistical uncertainty on the internal energy per atom is of the order of 5 K. For the B2 phase the estimated error bar is twice as large in the interval 600 K$\leqslant T\leqslant$900 K, temperatures at which the atomic exchanges are already important but still difficult to sample.

RESULTS

As a first step, we compute the $T=0$ K phase diagram of $Cu_xPd_{(1-x)}$ as a function of composition in a wide interval around $x=0.5$. For several $0.30\leqslant x\leqslant 0.70$, we compare the potential energy of the ordered B2 and random fcc alloy. In the B2 case, for $x\neq 0.5$ we start our computation by assuming that the majority element fully occupies one of the two cubic sublattices, while the excess concentration appears as anti-site defects on the other sublattice.

All systems are equilibrated at low T ($T=100$ K) by the Monte Carlo (MC) procedure described above (including atom pair exchanges) before their energy is minimized. The results for the excess energy of mixing at $T=0$, defined by

$$E_{mix}(x)=E(x)-xE(Cu)-(1-x)E(Pd),$$

[where $E(x)$, $E(Cu)$, and $E(Pd)$ are the cohesive energies per atom of the alloy and of the pure metals, respectively] are reported in Fig. 1.

It is apparent (and was already well known) that the potential energy gain in mixing Cu and Pd is the driving force for the stability of the B2 phase, which, being based on the bcc lattice, provides at $x=0.5$ the optimal hetero-coordination of each atom. By contrast, the same energy gain cannot be obtained by the fcc lattice, because, in this case, at $x=0.5$ it is impossible to surround each atom by a nearest neighbors' shell of hetero-atoms.

We observe that, despite the high degree of disorder in the fcc solid solution, non-negligible correlations do exist in the atomic distribution of the optimized structures, since at $x=0.5$ the fcc alloy with completely random distribution of Cu and Pd (i.e., produced in the same way as described above, but with random atom exchanges) has an energy 0.02 eV/atom higher than that of the annealed fcc sample.

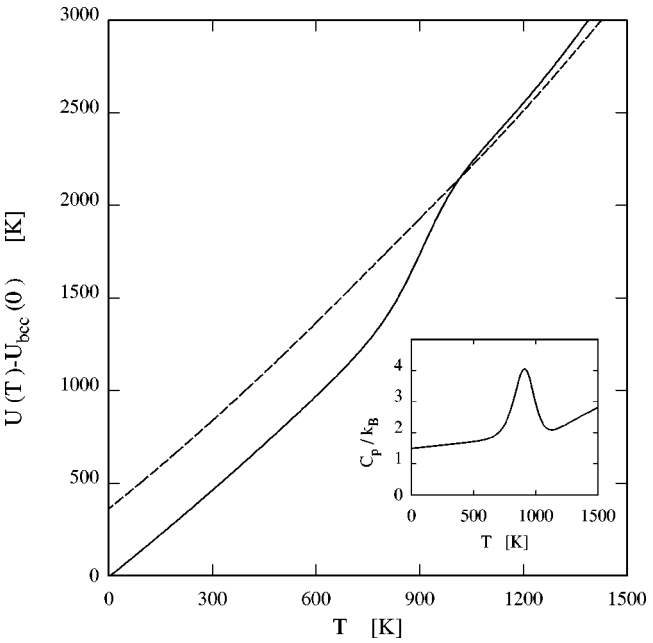

FIG. 2. Average potential energy (per atom) as a function of temperature at composition $x=0.5$. Full line: B2 phase; dash line: disordered fcc phase. The zero of the energy is set equal to the $T=0$ K energy of the B2 structure. Inset: constant pressure-specific heat of the B2 phase.

As apparent from Fig. 1, the EAM predicts the stability of the B2 phase at $T=0$ K for concentrations $0.31\leqslant x\leqslant 0.63$. This results is in qualitative agreement, but apparent quantitative disagreement with the experimental phase diagram: according to the data reported in Ref. 2, the B2 phase is stable for x between 0.42 and 0.72.[10] The reasons for this disagreement are discussed below.

As a second stage, we perform a series of simulations for the system at $0\leqslant T\leqslant 1500$ K, with the CsCl and disordered fcc structures. The internal energy as a function of temperature $U(T)$ is reported in Fig. 2. In the case of the bcc structure, $U(T)$ has a clear deviation from linearity starting from $\sim$700 K, corresponding to the onset of the order-disorder transition. The specific heat $C_p(T)$ of the B2 phase, computed by differentiation of a Padé fit for $U(T)$,[11] displays a peak centered at $T\sim 940$ K (See the inset of Fig. 2), that we identify with the order-disorder transition temperature for the bcc lattice (according to the data reported below, the bcc lattice is only metastable at this temperature). The fcc phase does not have such a sharp transition, and the corresponding $U(T)$ is almost linear over the entire temperature range.

The determination of the relative stability of the B2 and fcc phases requires the computation of their free-energy difference as a function of temperature. In particular, we need to evaluate the difference of their entropies, that we compute via the relation

$$S^{bcc}(T)-S^{fcc}(T)=S^{bcc}(T_0)-S^{fcc}(T_0)+\int_{T_0}^{T}\frac{C_p^{bcc}(T')-C_p^{fcc}(T')}{T'}dT'. \quad (2)$$

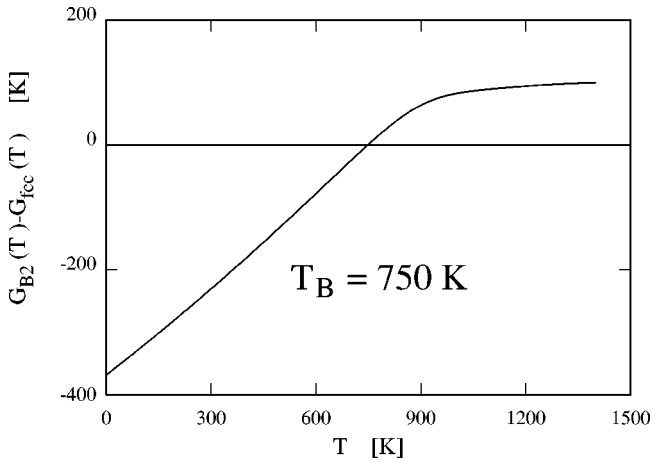

FIG. 3. Difference in the Gibbs free energy (per atom) of the B2 and disordered fcc phases as a function of temperature at composition $x=0.5$.

Since the specific heats of both phases tend to the same harmonic limit at low T, Eq. (2) is well behaved at any temperature, and provides a well-defined entropy difference for $T \rightarrow 0$ K, even in the classical mechanics formulation underlying our simulation results. For the same reason, the entropy difference at $T=0$ K can be attributed to the mixing contribution only. The consistent choice of this integration constant requires some care, because at low temperature the distribution of Pd and Cu on the fcc lattice is neither ordered nor fully disordered. However, we can assume that the mixing is fully random at $T=1500$ K, and, therefore, we can set $S_{mix}^{fcc}(1500\ \mathrm{K}) = -K_B[x \log x + (1-x)\log(1-x)]$. Then, the mixing entropy at any temperature lower than $T=1500$ K is obtained by computing the average potential energy $U^{fcc-rand}(T)$ for an artificial fcc phase with random exchanges of the atoms, and using a relation analogous to Eq. (2):

$$S_{mix}^{fcc}(T) - S_{mix}^{fcc-rand}(T) = S_{mix}^{fcc}(1500\ \mathrm{K}) - S_{mix}^{fcc-rand}(1500\ \mathrm{K}) - \int_T^{1500\ \mathrm{K}} \frac{C_p^{fcc}(T') - C_p^{fcc-rand}(T')}{T'} dT'$$

where, for any T, $S_{mix}^{fcc-rand} = -K_B[x \log x + (1-x)\log(1-x)]$, and, as explained above, also $S_{mix}^{fcc}(1500\ \mathrm{K})$ is assumed to be equal to $S_{mix}^{fcc-rand}$. These considerations allow us to compute $S^{bcc}(0\ \mathrm{K}) - S^{fcc}(0\ \mathrm{K})$, and to use eq. (2) with $T_0 = 0$ K.

The results for the Gibbs' free-energy difference $[\Delta G(T)]$ of the B2 and random-fcc phases are reported in Fig. 3: the conspicuous potential energy advantage of the B2 phase at $T=0$ is progressively compensated by the mixing entropy of the fcc alloy, which is the major reason for the linear behavior of $\Delta G(T)$ at low T. The compositional disordering of the bcc-based alloy, starting at $T \sim 700$ K, slows down the free-energy gain of the random fcc phase, but it comes too late to prevent the crossing of the B2-random fcc free energy that occurs at $T_B = 750$ K. Considering the simplicity of the EAM model, this result is in surprisingly good agreement with the experimental transition temperature of 770 K at $x=0.5$

The computation shows that the transition is weakly first order, with a minor volume change $(2[V^{B2} - V^{fcc}]/[V^{B2} + V^{fcc}] = 0.1\%)$, and a significant discontinuity in the constant pressure-specific heat $(2[C_p^{B2} - C_p^{fcc}]/[C_p^{B2} + C_p^{fcc}] = 0.25)$.

To check the validity of this description of the transformation, we performed extensive MC simulations for $T \geqslant T_B$ upon removing the constraint of fixed shape for the simulation box, starting from both the bcc and the fcc lattices. Over simulation runs of considerable length ($20\ 10^6$ single-atom MC steps), we do not observe the spontaneous transformation of one structure into the other, suggesting that the two phases are separated by a sizable free-energy barrier. To evaluate this barrier, we reintroduced the constraint of fixed shape for the simulation cell, and we performed a new series of simulations for tetragonal boxes with three values of the c/a ratio ($c/a = 1.1$, 1.2, and 1.3) intermediate between the bcc ($c/a=1$) and the fcc ($c/a=\sqrt{2}$) cases. The free-energy difference of these artificial phases with respect to the B2 and random-fcc structures is evaluated in complete analogy with the procedure described above. This computation confirms the presence of a free-energy barrier separating the B2 from the random-fcc phase, that at T_B is equal to 80 K per atom, and never becomes smaller than 50 K over the interval $T_B \leqslant T \leqslant 1500$ K.

As a final stage of our computational study, we investigate the dependence of the transition temperature on composition x. On the one hand, it is apparent already from Fig. 1 that the potential energy advantage of the B2 phase decreases rapidly in moving away from the $x=0.5$ composition. On the other hand, also the mixing entropy that stabilizes the random fcc structure has a maximum at the stoichiometric ($x=0.5$) composition, and it is not obvious which contribution will prevail at $T \neq 0$ and $x \neq 0.5$. Explicit simulations (following the same procedure of the $x=0.5$ case) show that the energy dependence on x is, by far, the dominant factor. More precisely, the decomposition of thermal effects into a mixing contribution and a remainder (due to the phonons), shows that the phonon contribution to the entropy and to the average potential energy is rather similar in all the phases involved, and, to first approximation, the transition temperature is determined by the equality: $T_B(x) S_{mix}^{fcc}(x, T=0\ \mathrm{K}) = U^{fcc}(x, T=0\ \mathrm{K}) - U^{B2}(x, T=0\ \mathrm{K})$. Moreover, since the dependence of mixing entropy on concentration is very weak around $x=0.5$, the transition temperature follows closely the behavior of the potential energy difference $\Delta U(x) = U^{fcc}(x, T=0\ \mathrm{K}) - U^{B2}(x, T=0\ \mathrm{K})$. For instance, at $x=0.58$, which corresponds to the highest transition temperature measured by experiments, the computed T_B is already reduced to 300 K, in apparent disagreement with the experimental data.

DISCUSSION

The analysis of the computational results shows, at first, that the EAM is remarkably successful in reproducing the qualitative features observed in the experimental phase diagram: the B2 phase is stable at low temperature around x

$=0.5$, and transforms with increasing temperature to the disordered fcc structure. Moreover, as described in the appendix, the stability of the $L1_2$ phase at $x=0.75$ is also reproduced by EAM, with a critical temperature for the order/disorder transition in qualitative agreement with the experimental result. In both cases, the driving force stabilizing the ordered structures is the positive heat of mixing of Cu and Pd, favoring the optimal alternation of these two elements in the alloy.

However, if we look more in detail into the comparison of the computational with the experimental data, we see that EAM is unable to reproduce the maximum in the transformation temperature at $x\sim0.58$, and, moreover, the temperature range of stability for the B2 phase is somewhat underestimated. More precisely, we find that the bell-shaped region of the $(x-T)$ plane in which the B2 phase is predicted to be stable by EAM is centered around $x=0.5$, and covers a smaller area than the corresponding region reported in the experimental phase diagram.

In focusing on these points of disagreement, it is important to identify the problems that are intrinsic to the EAM formulation, and those that, instead, could be eased by a better parametrization of the potential. For instance, the parametrization of Ref. 4, covering a wide set of different alloys, underestimates the mixing enthalpy of Cu and Pd by nearly 25% (See Table III in Ref. 4). A better parametrization for the Cu_xPd_{1-x} system (easily achieved by changing the single parameter determining the alloy mixing properties) could bring the maximum transition temperature in better agreement with the experimental result for both the $x=0.5$ and $x=0.75$ case.

More important is the problem related to the asymmetry of the stability region around $x=0.5$, that is not quantitatively reproduced by the EAM formulation, and does not seem to be affected by any of the parameters defining the potential of Ref. 4. Previous *ab-initio* computations[3] reveal that the electronic structure of Cu_xPd_{1-x} alloys is fairly complicated, and the electronic energy is affected by a variety of factors, including Fermi surface effects, which are strongly dependent on the band filling (i.e., on x), relativistic effects (mainly spin-orbit interactions), etc. These features are not, and cannot be, fully included in a simple model like EAM, that implicitly assumes a spherical Fermi surface and a schematic description of the electronic density of states.

However, the inclusion of these effects into slightly more sophisticated models (like the modified EAM,[12] the corrected EAM,[13] or the EAM including low-order moments of the electron density of states[14]) is possible, at least to some degree of approximation. Then, the bainitic transformation in Cu_xPd_{1-x}, described fairly well by the zero-order model, but displaying also sizable differences with the experimental data, could provide an ideal testing ground for the extension of these methods to alloys.

ACKNOWLEDGMENTS

We thank E. Bruno and B. Ginatempo for useful discussions.

APPENDIX

To complete the overview of the phase diagram of Cu-Pd, we investigated the transition from the $L1_2$ phase to the disordered fcc alloy for $x=0.75$. The simulation has been performed following exactly the same method described above, assuming a cubic simulation box with 864 atoms, and a variable volume to enforce the $P=0$ condition. The resulting potential energy U displays, as a function of T, a clear linear behavior both at low and at high temperatures, with a crossover starting at $T\sim400$ K and culminating at $T\sim500$ K. The specific heat, obtained by differentiating a Padé fit for $U(T)$, has a broad but apparent peak centered at $T=470$ K, that we identify with the order-disorder transition temperature. This result has to be compared with the experimental phase diagram, displaying a transition temperature of 730 K at $x=0.75$, and a stability region for the $L1_2$ phase centered at $x\sim0.82$, with a maximum transition temperature of 770 K.

[1] M. S. Daw and M. I. Baskes, Phys. Rev. Lett. **50**, 1285 (1983); Phys. Rev. B **29**, 6443 (1984).
[2] M. Hansen, *Constitution of Binary Alloys* (McGraw-Hill, New York, 1958); H. Baker, *et al.*, *Alloy Phase Diagrams* (ASM International, Materials Park, OH, 1992).
[3] See: E. Bruno and B. Ginatempo, Europhys. Lett. **42**, 649 (1998) for $x=0.5$; and Z. W. Lu, S.-H. Wei, and A. Zunger, Phys. Rev. B **45**, 10 314 (1992) for $x=0.75$.
[4] M. Foiles, M. S. Daw, and M. I. Baskes, Phys. Rev. B **33**, 7983 (1986).
[5] M. P. Allen and D. J. Tildesley, *Computer Simulation of Liquids* (Clarendon, Oxford, 1989).
[6] H. C. Andersen, J. Chem. Phys. **72**, 2384 (1980).
[7] M. Parrinello and A. Rahman, J. Appl. Phys. **52**, 7182 (1991).
[8] E. C. Bain, Trans. AIME **70**, 25 (1924).
[9] The acceptance ratio has been kept between 0.35 and 0.5 at all temperatures.
[10] The quoted experimental results refer to a temperature slightly above room temperature, while the computational data refer to $T=0$ K. However, at low T, the dependence of the phase boundaries on temperature is very weak.
[11] The internal energy is approximated by the ratio of two polynomials in T, whose degree is 3 for the numerator, and 2 for the denominator.
[12] M. I. Baskes, J. S. Nelson, and A. F. Wright, Phys. Rev. B **40**, 6085 (1989).
[13] T. J. Raeker and A. E. De Pristo, Phys. Rev. B **39**, 9967 (1989).
[14] S. M. Foiles, Phys. Rev. B **48**, 4287 (1993).